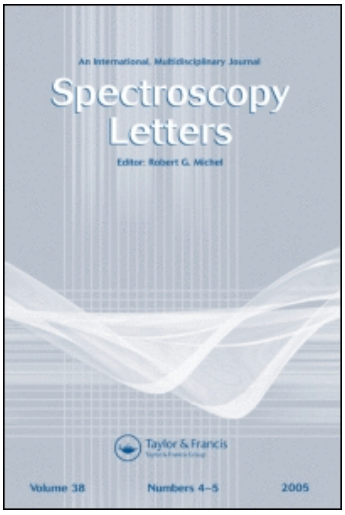

Spectroscopy Letters
Publication details, including instructions for authors and subscription information:
http://www.informaworld.com/smpp/title~content=t713597299

Multicenter Structure and Dynamical Processes in the Rare Earth Doped Garnet and Sesquioxide Laser Crystals and Ceramics

V. Lupei[a]; A. Lupei[a]; A. Ikesue[b]
[a] National Institute of Laser, Plasma and Radiation Physics, Bucharest, Romania [b] World Lab Co. Ltd., Nagoya, Japan

Online publication date: 30 July 2010

To cite this Article Lupei, V. , Lupei, A. and Ikesue, A.(2010) 'Multicenter Structure and Dynamical Processes in the Rare Earth Doped Garnet and Sesquioxide Laser Crystals and Ceramics', Spectroscopy Letters, 43: 5, 357 — 372
To link to this Article: DOI: 10.1080/00387010903329409
URL: http://dx.doi.org/10.1080/00387010903329409

Spectroscopy Letters, 43:357–372, 2010

ISSN: 0038-7010 print/1532-2289 online
DOI: 10.1080/00387010903329409

Taylor & Francis
Taylor & Francis Group

Multicenter Structure and Dynamical Processes in the Rare Earth Doped Garnet and Sesquioxide Laser Crystals and Ceramics

V. Lupei[1], A. Lupei[1], and A. Ikesue[2]

[1]National Institute of Laser, Plasma and Radiation Physics, Bucharest, Romania
[2]World Lab Co. Ltd., Nagoya, Japan

ABSTRACT This article presents new data on multicenter structure of the optical spectra and of emission dynamics of the doping ions in various types of crystalline and polycrystalline cubic laser materials (garnets, sesquioxides). It is inferred that the satellite structure of the active ions is induced by crystal field perturbations inside the near neighbor associations of the active ion with specific defects of the host lattice (*P*-type satellites independent on doping concentration) or with other active ions (*M*-type satellites dependent on doping concentration). Such satellite structures are described for various rare earth ions; including Nd^{3+}, Pr^{3+}, Er^{3+}. In case of the garnet crystals, both types of satellites are present, and the satellites *P* can be connected with departures from stoichiometry; in garnet ceramics, they are much less intense. In contrast, the structures of *M* satellites are similar in garnet crystals and ceramics, indicating similar distribution of the doping ions in the host matrix. The luminescence spectra of these materials are influenced by the emission quantum efficiency of the various centers. In the case of sensitized materials, the mutual crystal field perturbations could modify the absorption spectra on both the sensitizer ions. In the case of materials with charge compensation, the electric charge disordering determined by the process of compensation strongly influences the optical spectra of the doping ions and their distribution. The relation between the global spectroscopic properties and those measured by microscopic methods is also considered. The connection between the fabrication process, structure, spectroscopic, and laser emission properties is shown and it is inferred that the multicenter structure of the spectra, together with emission dynamics, can be an efficient tool for investigating the microstructure of the laser materials, for optimization of laser properties, or for tailoring new laser materials.

KEYWORDS laser ceramics, laser crystals, laser materials, multicenter structure, optical spectra

Received 19 August 2009; accepted 11 September 2009.

Address correspondence to V. Lupei, Solid-State Quantum Electronics Lab, Atomistilor Str 409, Bucharest-Magurele 077125, Romania. E-mail: lupei_voicu@yahoo.com

1. INTRODUCTION

The positions and intensities of lines in the optical absorption and emission spectra of the rare earth (RE^{3+}) active ions in the laser materials are essentially determined by the crystal field interaction at the substituted site. Crystalline laser materials used in the construction of lasers with a defined wavelength must grant unique structural centers for the doping ions, with well defined optical spectra, and materials that provide for substitution at a unique crystallographic site. The optical spectra of the RE^{3+} ions in such materials have sharp absorption and emission lines with high peak cross-sections. However, the high-resolution spectra of these materials often show structures of spectral satellites or/and inhomogeneous broadening that suggest the existence of a variety of centers with a slightly different crystal field interaction (multicenter structure). The multicenter satellite structures reflect the existence of discrete crystal field perturbations caused by a certain degree of structural disorder in the near coordination spheres around the doping ion. The structural disorder can be introduced by structural defects of the host material such as the inversion of occupancy of the cationic sites or the excess of some cationic species on the expense of others resulting in non-stoichiometric composition; the occurrence of such defects is influenced by the fabrication process, especially by the thermal regime. The statistical ensembles of doping ions in near sites, determined by their distribution in the crystallographic sites of the host material, can also induce structural disorder in the cationic coordination spheres around the doping ion and the effect depends on the doping concentration C_{RE}.

A special case is presented by the laser materials in which the doping ion substitutes a host cation of different valence; in such a case, the compensation of the difference of electric charge is necessary and this can be accomplished by various intrinsic mechanisms such as interstitial anionic or cationic species, ionic vacancies, or by extrinsic means, such as co-doping with charge-compensator ions. The various modalities of placement of the charge compensator with respect to the laser active ion induce a structural disorder and the global effect is strongly influenced by technological details. The differences of electric charge in the near coordination spheres induced by the charge-compensators could induce crystal field perturbations at the doping ion site stronger than those caused by the differences in ionic size. Moreover, function on the local difference of charge introduced by the compensator, the charge compensation processes could modify the distribution of the doping ions, leading to their clustering in pairs or more complex ensembles in the vicinity of compensator.

In special situations, such as tunable or ultra-short pulse laser emission, materials with inhomogeneous broadening of the absorption or emission lines are desired. These materials could contain quasi-continuous distribution of the structure of the substitution site, such as for glasses, or they could offer several discrete and well defined crystallographic sites whose optical spectra are close enough to coalesce. Special cases are the compositionally disordered crystalline materials, which have a defined crystallographic structure, usually with several cationic sites that can be occupied by various species of ions of different ionic radius or electric charge. In these systems, the doping ions occupy a defined unique crystallographic site but the composition of the coordination spheres formed by the surrounding ions around the doping ions could be different, leading to specific differences in the crystal field potential.

Because of the strong dependence of the crystal field interaction on distance, the effect of the structural disorder on the optical spectra is determined by the distribution of disorder near the laser ion. In several instances, the perturbation could also be anisotropic. The discreteness of the crystalline lattice determines a chain of discrete crystal field perturbations that could be resolved in the optical spectra leading to multicenter structure of the lines. The unresolved perturbing effect of the farther sites results in inhomogeneous broadening of lines; in many cases, the broadening could smear the multicenter structures of the spectra, resulting in broad, sometimes multi-peaked optical bands.

The distribution of the structural disorder can also influence the dynamic properties of emission by modification of the radiative lifetime of the various centers or by specific manifestation of the energy transfer processes, leading to further personalization of the centers. These static and dynamic effects of the structural disorder influence the laser properties

(pump absorption, emission) of the laser material. At the same time, the investigation of these specific effects of the structural disorder could contribute to elucidation of the structure of the laser material and of the distribution of the doping ions and defects.

An important emerging class of laser materials is that of the transparent polycrystalline materials produced by ceramic techniques.[1–8] There are several such ceramic techniques, but for all of these the maximum temperature corresponds to the final sintering step and is by about 400°C to 700°C smaller than for the crystal growth from melt. The solid-state process of formation of ceramics enables a larger compositional versatility compared with crystal growth from melt, particularly the possibility to incorporate much higher concentrations of doping ions. Nevertheless, the thermal regime of fabrication and the granular structure of these ceramics could influence the occurrence of specific intrinsic defects of the material and the distribution of the doping ions and of defects.

Although the multicenter structure of the optical spectra of the laser materials was described largely in the literature, few papers have attempted to relate the spectral satellites with the structural properties of the material; moreover, sometimes conflicting results and models are presented. This paper introduces new data and provides a deeper discussion of the multicenter structure of the optical spectra and of dynamic effects in single crystals and transparent polycrystalline ceramics of RE^{3+}-doped cubic garnet and sesquioxide laser materials. The implication of this multicenter structure of optical spectra on the structural models of the laser materials and on their laser properties is also discussed.

2. EXPERIMENTAL TECHNIQUES

The samples under investigation are RE:$Y_3Al_5O_{12}$ (YAG) and Nd:$Gd_3Sc_2Ga_3O_{12}$ (GSGG) single crystals or transparent ceramics and RE^{3+}-doped cubic sesquioxide ceramics. The crystals are home grown by Czochralski technique or commercial samples, whereas the transparent polycrystalline materials are produced at the World Lab Co. Ltd. Nagoya-Japan, by the technique based on solid-state synthesis.[1,2] The spectroscopic investigation involves high-resolution optical absorption, lamp or laser-induced luminescence and luminescence decay under short-pulse excitation (10 ns) in the temperature range from 10 K to 300 K. Since the transverse section of probe or exciting beam in these experiments is much larger than the size of the ceramic grains, these measurements characterize the global behavior of the samples.

3. EXPERIMENTAL RESULTS

3.1. Laser Materials without Charge Compensation

3.1.1. Multicenters in the Absorption Spectra of Rare Earth Doped Garnet Single Crystals and Ceramics

The garnets are cubic materials, of general formula $A_3B_2C_3O_{12}$, where A denotes ions large radius ions (such as Y^{3+} or Gd^{3+}) in dodecahedral sites with eightfold oxygen coordination, whereas B and C are smaller ions in six-fold coordinated octahedral sites (B=Al^{3+}, Ga^{3+}, Sc^{3+}) or in fourfold tetrahedral sites (C=Al^{3+} or Ga^{3+}). The doping RE^{3+} ions substitute the large ions A. A major representative of this family is $Y_3Al_5O_{12}$ (YAG). High-quality Nd:YAG single crystals can be produced by Czochralski technique but the quite low (~0.18) segregation coefficient leads to non-uniform doping along the direction of growth and to limited Nd concentration (1.2 to 1.5 at.% Nd). This shortcoming can be avoided by using polycrystalline garnet materials produced by ceramic techniques. Basically, there are two classes of ceramics techniques, the technique with solid-state synthesis of the final compound from the elementary oxides, followed by isostatic compression to reduce the density of pores and by final vacuum sintering[1,2] and techniques with wet-chemistry synthesis of a precursor that is thermally reduced and transformed into nanocrystalline powder which is sintered by a nanotechnology process.[3] Whereas in the case of coarse-grained ceramics a sintering aid to control the grain growth could be required, for the fine-grained ceramics the sintering process is controlled by the large surface energy of the nanoparticles. The average size of the ceramic grains is of tens of microns in the solid-state method (coarse-grained ceramics) and of several microns in the ceramics based on the

nanotechnology process (fine-grained ceramics). Nevertheless, the granular structure of the ceramics poses basic questions concerning the quantum states of the doping ions, the variety and nature of the structural centers of the doping ions, the distribution of the doping ions at the available crystal sites. Many of these aspects have been discussed in literature and are presented in review papers.[9–11] Similar to the case of the Nd:YAG single crystals,[12,13] the high-resolution spectroscopy can be very efficient tool in investigation of these characteristics in Nd:YAG ceramics. The high-resolution spectroscopy is performed at low temperatures, usually ~10 K, when the lines are sharp and enable good resolution.

High-resolution absorption spectroscopy of the Czochralski-grown Nd:YAG crystals revealed two types of spectral satellites, a group of equally intense satellites P_i, whose intensity was independent on the Nd concentration C_{Nd} and satellites M_i, whose intensity was dependent on C_{Nd}.[12–17] Figure 1 shows the satellite structure of the low temperature (15 K) absorption line $^4I_{9/2}(1) \rightarrow {}^4F_{9/2}(1)$ of 1.5 at% Nd:YAG crystal. The occurrence of the *Pi* satellites in these crystals was linked with the anisotropic crystal field perturbing effect of the excess of A ions in the melt-grown garnet crystals, that enter in the octahedral sites specific to the ions B (when B=Al or Ga) in the garnet structure.[18,19] The satellites P_i are present in the absorption spectra of all RE^{3+} ions in YAG crystals and the number of spectrally resolved satellites P_i depends on the electronic transition. It was shown[17] that the maximum number of P_i satellites is four and this was linked with the four sites of the nearest neighbor (n.n.) coordination sphere of octahedral sites around the dodecahedral site occupied by RE^{3+}. In the case of the Nd-doped YAG transparent ceramics, the relative intensity of the P_i satellites is much lower than for the melt-grown crystals and this was linked with the lower (by about 300 K) fabrication temperature.[20–23] The structure of C_{Nd}-dependent satellites M_i in the Nd-doped crystals contains a single resolved satellite or several satellites whose relative intensity is not equal, their ratio being dependent on the crystalline structure of the host material. The relative intensity of each M satellite with respect to the global intensity increases linearly with C_{Nd} up to the maximum concentration available for crystals (~2.5 at.%).[12] The structure of satellites M_i in Nd:YAG ceramics was similar to that observed in the melt-grown crystals (a clearly resolved satellite M_1 and a satellite M_2 twice intense as M_1, which in some transitions is split into two equally intense components) and their relative intensity continued to increase practically linearly with C_{Nd} to 9 at.% Nd.[20–23] In several transitions the satellite M_1 shows tendency of splitting indicating superexchange coupling between the corresponding Nd ions. At very high Nd concentrations new satellites, more shifted from the N line and with the intensity increasing more than linearly with C_{Nd} become apparent, such as the T satellite in the absorption spectrum of the 6.6 at.% Nd:YAG ceramic shown in Fig. 2.

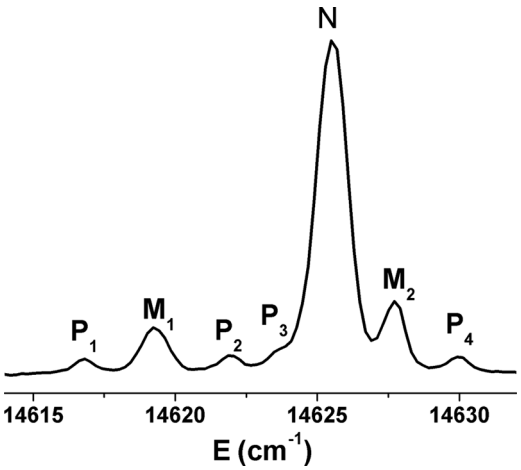

FIGURE 1 Satellite structure of $^4I_{9/2}(1) \rightarrow {}^4F_{9/2}(I)$ absorption line at 15 K in 1.5 at.% Nd:YAG crystal.

The previous measurements on YAG single crystals doped with Er in concentrations up to 100 at.% revealed in the $^4I_{15/2} \rightarrow {}^4S_{3/2}$ absorption line a clearly resolved four-line structure of P_i satellites.[17] As shown in Fig. 3, at low C_{Er} these satellites lines are well defined and sharp, but with increased Er concentration a new line shows near each P_i satellite: their intensity increases linearly with C_{Er}, while that of the original satellite decreases. Thus, at 100 at.% Er the structure of original P_i satellites is completely replaced by four $P_i(Er)$ satellites, indicating that in case of the ErAG crystals a non-stoichiometric structural defect similar to YAG occurs with about the same probability. Our new measurements on Er-doped YAG ceramics shows that, similar to the Nd:YAG ceramics, the intensities of the P_i and $P_i(Er)$ satellites become very small. No resolved spectral satellites M were observed in the Er: YAG single crystals or ceramics, although inhomogeneous

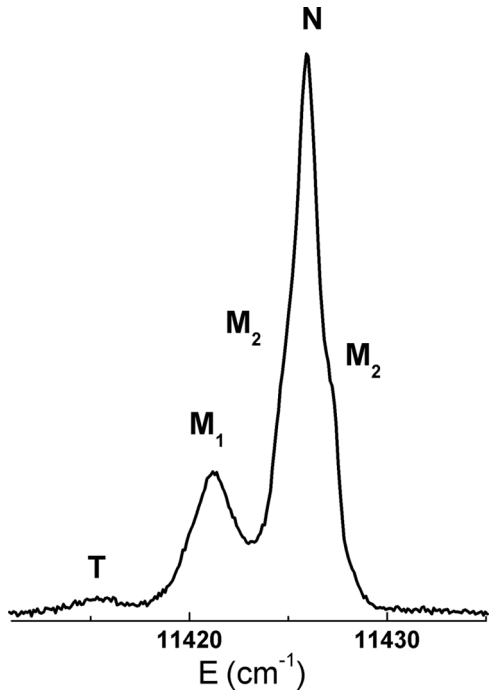

FIGURE 2 Satellite structure of $^4I_{9/2}(1) \rightarrow {}^4F_{3/2}(I)$ absorption line at 15 K in 6.6 at.% Nd:YAG ceramic.

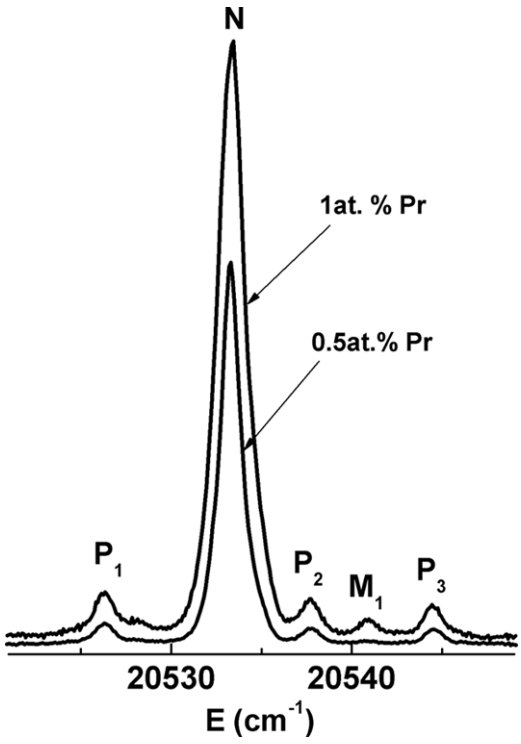

FIGURE 4 Satellite structure of $^3H_6(I) \rightarrow {}^3P_0$ absorption line at 15 K of Pr:YAG crystal.

concentration-broadening of the lines is obvious. The high-resolution absorption spectra of Pr^{3+} in Czochralski grown YAG single crystals shown in Figure 4 manifest similar structure of P_i satellites as for Nd or Er doping, whereas in ceramics these lines are again very weak. The relative intensity of the M_i satellite in the Pr:YAG crystals and ceramics is similar for a given Pr concentration.

In case of the non-Kramers ions such as Tm^{3+} the electric dipole transitions between the Stark levels of several manifolds, such as that between the first Stark level of the ground manifold $^3H_6$ and the second Stark level of the excited manifold $^3H_4$, are forbidden in the D_2 symmetry of the dodecahedral site of garnets, and this complicates the analysis of the energy level structure of these materials. However, the Tm doped Czochralski-grown YAG or GGG crystals show weak lines in the spectral region where transitions would be normally forbidden.[24,25] These lines are interpreted as *P* satellites and their presence indicates the lowering of the local symmetry from the original D_2 group due to crystal field perturbation; they proved instrumental in construction of accurate energy level schemes for Tm^{3+} in GGG and YAG.[25,26] Our new measurements did not show such lines in the Tm:YAG ceramics, confirming their connection with the departure from stoichiometry in the YAG crystals. Apparently, the lowering of symmetry in case of the statistical ensembles of Tm^{3+} ions in near lattice sites is not strong enough to grant sizable intensity for the *M* satellites in these forbidden transitions.

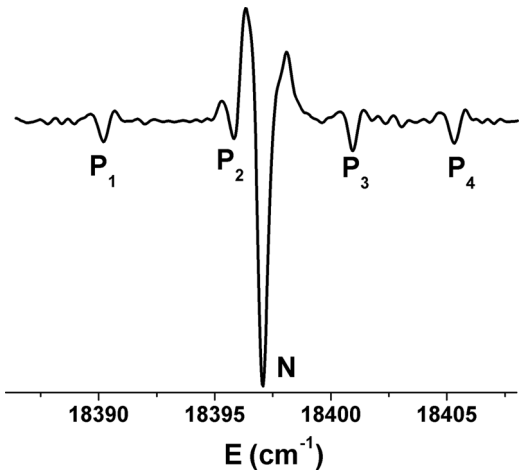

FIGURE 3 Satellite structure of $^4I_{15/2}(1) \rightarrow {}^4S_{3/2}(I)$ absorption line (second derivative) at 15 K in 1 at.% Er:YAG ceramic.

The satellite structure is best resolved in the absorption line to the first Stark component of the upper manifold. The positions of the P_i and M_i satellites in the low-temperature absorption spectra of

TABLE 1 The Shift of the Spectral Satellites from the Main Line *N* in the 15 K Absorption Spectra of Various Trivalent Rare Earth Ions in YAG Crystals

System	Main line N, cm^{-1}	Satellites P_i, cm^{-1}	Satellite M_1, cm^{-1}
Nd:YAG $^4I_{9/2}(1) \rightarrow {}^4F_{3/2}(1)$	11425.5	−16.5; −1.3; +5.3	−5
Nd:YAG $^4I_{9/2}(1) \rightarrow {}^4F_{7/2}(1)$	14626.5	−10; −4; +3.5	−7.5
Pr:YAG $^3H_4(1) \rightarrow {}^3P_0(1)$	21544	−7; +4.3; +10.6	+7.6
Pr:YAG $^3H_4(1) \rightarrow {}^3P_1(1)$	21045	−23; −14; +15	+8
Er:YAG $^4I_{15/2}(1) \rightarrow {}^4S_{3/2}(1)$	18397	−7; −1;+4; +8	
Er:YAG $^4I_{15/2}(1) \rightarrow {}^4I_{9/2}(1)$	15284	+6; +9	

several rare earth ions in YAG single crystals and ceramics are given in Table 1. The optical spectra of Nd:GSGG single crystals and ceramics are similar.[27]

The P_i satellites are absent and the satellites M_i are identical in both materials and show as shoulders on the absorption line of the main center *N*. The second derivative of the absorption lines shows that the structure of satellites M_i in Nd:GSGG is similar to Nd:YAG: in several electronic transitions the satellite M_2 is split in two components and their global intensity is practically double to that of satellite M_1.

3.1.2. Spectral Satellites in the Absorption Spectra of Rare Earth Doped Cubic Sesquioxides

The cubic sesquioxides R_2O_3 (R=Gd, Y, Sc) have a bixbyite structure, with two cationic sites surrounded by six oxygen ions, of C_2 and C_{3i} local symmetry, in proportion 3:1. The RE^{3+} ions can substitute both these sites,[28–30] but the dipole–dipole transitions between the energy manifolds are forbidden for the inversion centers of C_{3i} symmetry, and the magnetic dipole transitions are allowed for both centers only for transitions with $\Delta J = 0, \pm 1$. Thus the presence of the both centers is seen in the optical spectra only for transitions satisfying these conditions, usually placed in infrared. The high density and the strong packing of cationic sites and the short cation–cation distances in these materials favor strong crystal field interactions and efficient energy transfer between the doping ions.

The crystal growth of cubic sequioxides is difficult because of the very high melting temperature (~2420°C),[31,32] but ceramic techniques[2,33] could now offer highly transparent sesquioxide polycrystalline materials. No investigation of the satellite structure was reported for RE^{3+} in cubic sesquioxide single crystals, although satellites of high relative intensity and well resolved could be expected due to perturbations inside the statistical ensembles (pairs, triads, etc.) of doping ions in the n.n. sites, favored by the tight packing of the cationic sites. However, the 15 K absorption spectra of the Nd-doped Y_2O_3 ceramics revealed clearly resolved satellites whose intensity increases with the doping concentration (*M*-type satellites) and these were attributed to perturbations inside the n.n. pairs of Nd ions.[34] At the same time, the unresolved effect of the perturbations in the farther pairs induces strong concentration-dependent asymmetric inhomogeneous broadening of the absorption lines. In the RE-doped Sc_2O_3 ceramics investigated in this work, the spectral shift of the M_i satellites from lines *N* is much larger than for YAG, up to 40 cm^{-1} for Nd^{3+} and up to 13 cm^{-1} or Er^{3+}. In several sesquioxide ceramics investigated in this work additional lines, similar to those reported for Y_2O_3 ceramics[35] are present and they could be tentatively linked with the HfO_2 sintering aid used in the fabrication process.

3.1.3. Spectral Satellites in Laser Materials with Multiple Doping

Sensitization of emission by co-doping the laser materials with two species of ions (activator A and sensitizer S) assumes efficient non-radiative energy transfer from S to A, which is favored by short S-A distances and tight packing of the A ions around S. Placement of the ions A close to S could perturb the crystal field at each other's site, leading to resolved spectral satellites that could influence the absorption properties of S and the emission properties of A; such satellites have been observed in many sensitized crystalline laser materials such as garnets. However, no investigation of such processes in the

crystalline RE doped cubic sesquioxides was reported, although these materials show very good qualities for investigation of sensitized emission. This paper investigates the effect of sensitization in ceramic sesquioxide materials on the optical spectra of the doping ions. In case of (Nd, Yb):Sc_2O_3 ceramics, where Nd^{3+} acts as sensitizer and Yb^{3+} as activator[36] the presence of Yb^{3+} leads to apparition in the Nd^{3+} spectra of a satellite whose intensity increases with Yb concentration and competes with the line *N*. In case of the Nd^{3+} $^4I_{9/2}(1) \rightarrow {}^4F_{5/2}(1)$ absorption shown in Fig. 5 and in the absorption $^4I_{9/2}(1) \rightarrow {}^4F_{3/2}(1)$ this satellite is placed $\sim 13.5\,cm^{-1}$ (i.e., $\sim 0.9\,nm$) above the line corresponding to the main line *N* and above ~ 5 at.% Yb it dominates the absorption. This shift is accompanied by strong C_{Yb}-dependent inhomogeneous broadening of the absorption lines. These modifications of the absorption spectra could influence the laser diode pumping properties. In several transitions, this shift could be much larger, for instance in transition $^4I_{9/2}(1) \rightarrow {}^4F_{9/2}(1)$ the shift approaches $30\,cm^{-1}$. Similar situation is observed in case of Sc_2O_3 ceramics co-doped with Yb^{3+} (S) and Er^{3+} (A) or with Yb^{3+} (S) and Pr^{3+} (A).

3.1.4. Structural Models for the Spectral Satellites in the Absorption Spectra of Rare Earth Doped Garnets and Sesquioxides

These examples indicate a clear connection between the composition and structure of the laser material and the structure (number and relative intensities) of the spectral satellites in the absorption spectra of the doping rare earth ions. It is thus obvious that these satellites are linked with the discrete chain of crystal field perturbations induced by specific defects of the host material (the P_i satellites in case of garnets) localized in the close vicinity of the doping ion or by those manifested inside the statistical ensembles of doping ions in near lattice sites (satellites M_i in garnets and sesquioxides). Although the distortion of the crystalline lattice by substitution with doping ions or defects is extended over several anionic and cationic coordination spheres, we consider that the source of perturbation is localized at the site of the perturbing center. Since the crystal field perturbations depend on the distance to the laser active ion, the perturbations coming from the various coordination spheres would be different. The perturbing centers could occupy *n* out of the *m* sites in each coordination sphere. The relative intensities of the spectral satellites with respect to each other or to the total intensity of lines of an electronic transition depend on the distribution of the doping ions and defects in the crystalline lattice. Thus, the observed satellites can be used to assess this distribution: a major condition is that the absorption cross-sections of all centers (unperturbed or perturbed) are equal, i.e., that the perturbation does not modify sizably the cross-sections.

The intensities of the lines corresponding to perturbed centers due to presence of *n* perturbing centers in the *m* available sites are determined by the concentration of the perturbing centers C_{mn} and by the oscillator strength of the corresponding satellite line f_{mn}, i.e., $I_{mn}^{(abs)} = C_{mn} f_{mn}$. In case of induced electric dipole transitions[37,38]

$$f_{mn} \propto \sum_{\lambda=2,4,6} \Omega_\lambda(m,n) \langle f^n J \| U^{(\lambda)} \| f^n J' \rangle^2 \qquad (1)$$

where $\Omega_\lambda(m,n)$ are the Judd-Ofelt parameters for the corresponding satellite, $U^{(\lambda)}$ is the unitary tensor operator of rank λ and $f^n J$ and $f^n J'$ denote the electronic manifolds of the ground electronic configuration $4f^n$ connected by the optical transition. The parameters Ω_λ are determined by the odd crystal field parameters $B_k^{(q)}$ with $k = \lambda \pm 1$. Since the perturbing centers are placed in the cationic coordinating spheres, the perturbations influence mainly the low-order terms in the crystal field potential, which are most sensitive to the distant contributions. Thus, in order to minimize the effect of the perturbations on the oscillator strengths for the various perturbed centers, transitions with $\langle f^n J \| U^{(2)} \| f^n J' \rangle \cong 0$ must be selected to cancel the effect of Ω_2. For these transitions the relative intensities of the satellites and of the main line will be strictly proportional to the relative concentrations of the corresponding perturbed and non-perturbed structural centers. At the same time, the relative concentrations of the various centers C_{mn} are proportional with the global concentration *C* of the perturbing center and with the probability of occurrence for the structural centers P_{mn} calculated in various structural and distribution models and thus the measured values could be used for validation of these models. In case of random

occupancy with equal probability p of n out of the m sites of a coordination sphere by the perturbing centers

$$P_{mn} = \frac{m!}{n!(m-n)!} p^n (1-p)^{m-n} \qquad (2)$$

For complete random occupation of all the available sites the probabilities p are equal for all coordination spheres available to perturbing centers and equal to their relative concentration C. The calculated matrix elements $\langle f^n J \| U^{(2)} \| f^n J' \rangle$ are tabulated[39] and some absorption transitions for which they are zero or close to zero are in case of Nd^{3+} the transitions from the ground manifold $^4I_{9/2}$ to the manifolds $^4F_{3/2}$, $^4F_{5/2}$, $^2P_{1/2}$, in case of Er^{3+} the transitions from the ground manifold $^4I_{15/2}$ to the manifold $^4S_{3/2}$, in case of Pr^{3+} the absorption $^3H_4 \rightarrow {}^3P_0$ and so on.

The analysis of the satellite structure in the optical absorption spectra of RE^{3+}-doped garnet single crystals and ceramics and cubic sesquioxide ceramics shows that:

- the measured intensities of the satellites P_i in the melt-grown YAG crystals correspond to the calculated intensities assuming that the perturbing centers are placed at random in the n.n. octahedral sites and their relative concentration is equal to that of excess of Y^{3+} ions: in the Czochralski-grown crystals the proportion of octahedral sites occupied by these ions is ~1.8%, whereas in ceramics this is by about an order of magnitude lower. This indicates that, whereas the YAG ceramics are close to the ideal garnet composition, the melt-grown crystals are in fact 1.8 at.% $Y(Al_{oct})$-doped YAG.
- the experimental relative intensities of the satellites M_1 and M_2 in garnets and M_1 in sesquioxides correspond to the calculated relative concentrations of n.n. and n.n.n. Nd pairs assuming random distribution of the RE ions even at high concentrations. The structure (number, positions, and relative intensities) of the satellites induced by the statistical ensembles of doping ions in near sites in case of the coarse-grained ceramics is similar to that measured for crystals. The concentration dependence of the intensity of satellites T observed in the highly doped Nd:YAG ceramics suggest that these correspond to triads of Nd ions in n.n. sites.
- co-doping with another ion (sensitized emission) induces new spectral satellites in the absorption spectra of the A and S ions. For the systems investigated in this work the intensity of the new satellites can be described assuming random placement of the S and A ions.
- the unresolved effect of the perturbations induced by the farther coordination spheres leads to strong asymmetric inhomogeneous broadening of the spectral lines.

3.1.5. Emission Decay Under Non-Selective or Selective Excitation

The presence of the satellites in the absorption spectra of RE ions in the laser materials enables investigation of the emission decay of the various perturbed centers under selective excitation. The decay measured with short pulse (~10 ns) selective excitation can be then linked to that under non-selective excitation. However, due to the closeness of the satellites and of the main line and to the inhomogeneous broadening at high doping concentrations, the selective excitation is not an easy task and special care must be taken in the experiment and in the analysis of data in order to avoid the interferences from various centers.

The earlier investigation of the non-selectively excited decay in Nd-doped garnets shows that the energy transfer among the Nd ions by the cross-relaxation $(^4F_{3/2}, {}^4I_{9/2}) \rightarrow (^4I_{15/2}, {}^4I_{15/2})$ induces a very fast drop in emission at the beginning of decay, followed by complex non-exponential dependence on time. This behavior was explained by mixed superexchange and dipole-dipole interaction between the Nd^{3+} ions.[12,40,41] The analysis of decay indicates that the distribution of Nd in the YAG crystal is random, in agreement with the data inferred from the absorption spectra. The selectively excited emission decay of the satellite M_1 is exponential, very fast, and practically independent of C_{Nd}; this indicates that the transfer is dominated by the strong superexchange couplimg inside the n.n. Nd pairs. The emission decay of satellite M_2 shows C_{Nd}-dependent departures from exponential, and it was inferred that the energy transfer inside of these pairs is determined by dipole–dipole interaction but still shows residual influence of the superexchange interaction. The selectively excited

emission of the unperturbed main center N shows C_{Nd}-dependent non-exponential decay slower than the global decay under non-selective excitation and without the fast drop at beginning of decay; this is consistent with the exclusion of the n.n and n.n.n. pairs from the ensemble of ions influencing the decay of this center. The differences of decay for the various centers determined by the perturbations inside the ensembles of Nd ions induce differences in their emission quantum efficiency. The quantum efficiencies can be calculated by taking into account the distribution of the acceptor ions around the donor ion for each center by methods similar to that used for the global decay;[13,41] thus, the quantum efficiency of the emission of centers M_1 is only ~0.4% from that of the unperturbed centers N.

The emission decay measurements on Nd:YAG ceramics in large C_{Nd} range (to 9 at.% Nd)[20–23] indicate that at low C_{Nd} the decay is similar to that reported previously for single crystals and the energy transfer parameters inferred form these measurements describe well the decay at C_{Nd} unavailable (to ~6–7 at.% Nd) for crystals, although at higher concentration the decay is slightly accelerated. Obviously, these decay measurements reflect the global behavior of the dynamics of emission from the whole excited volume and it would be expected that any presumed strong departures from a random distribution such as large regions with strongly enhanced C_{Nd} in ceramics would modify the dynamics of emission and the relative intensities of the satellites M_i. However, the similarity of the emission decay of Nd and of M satellite structure in the YAG single crystals and ceramics indicates that no strong large-scale deviations from the distribution of Nd in crystals takes place in case of the coarse-grained ceramics: although regions of enhanced concentrations at the grain boundaries could be present, the quite large ratio (volume/surface) of the grains will reduce the global effect. Similar behavior is observed in the emission decay of Nd in the GSGG crystals and ceramics: the decay is similar for both materials and can be described with the same energy transfer parameters for mixed superexchange and dipole–dipole interaction between the Nd ions.

Mixed interaction between the Nd ions is also observed for Nd doped Sc_2O_3 and Y_2O_3 ceramics.[34,36] For the Y_2O_3 ceramic, which can be doped to very high C_{Nd}, the decay could be described to ~3 at.% Nd with the energy transfer parameters measured at low C_{Nd}. At higher C_{Nd}, however, a new energy transfer process, which induces additional emission decay with time and C_{Nd} dependence characteristic to cooperative energy transfer between an excited Nd ion and a pair of Nd ions became evident.[42] Such new mechanisms of transfer were also observed in the decay of $^3H_4$ emission of highly doped Tm:Sc_2O_3 ceramic and in the decay of ($^4S_{3/2}$,$^2H_{11/2}$) level of Er:Sc_2O_3 ceramics. In the last case, this cooperative de-excitation induces emission from the $^4I_{3/2}$ level and the dynamics of this emission shows a rise-time consistent with the lifetime of $^4S_{3/2}$ emission; with increasing C_{Er} this dynamics is influenced by strong upconversion processes from $^4I_{13/2}$ and $^4I_{11/2}$, similar to those evidenced for Er:YAG,[43] which strongly complicates the analysis of decay. The absence of emission from the T satellite in Nd:YAG shows that for such processes the coupling between the excited donor ion and the acceptor Nd pair in n.n. position is dominated by superexchange, whereas for transfer to distant pairs the electric dipole coupling dominates.

The emission decay in case of sensitized emission reflects similar features as for the single doped systems, and enables characterization of the distribution of the activators around the donor ions. Thus, the investigation of emission decay of Nd in the (Nd, Yb) co-doped Sc_2O_3 and Y_2O_3 ceramics,[36,44] where Nd acts as sensitizer and Yb as activator indicates that the distribution of Yb ions around the Nd ions is random.

3.1.6. Luminescence Spectra

The presence of a variety of structural centers in the laser materials influences also the luminescence spectra of these materials. However, by difference from the absorption spectra, where the intensities of the lines are determined by the relative concentrations of the centers and by the corresponding oscillator strengths, in case of luminescence the relative intensities for the various centers depend also on the emission quantum efficiency for each center as well as on the efficiency of excitation; $I_{mn}^{(em)} \propto C_{mn} f_{mn} \eta_{qe}^{(mn)} \eta_{exc}^{(mn)}$. Thus, whereas for transitions with $\langle f^n J \| U^{(2)} \| f^n J' \rangle \cong 0$ the absorption spectra

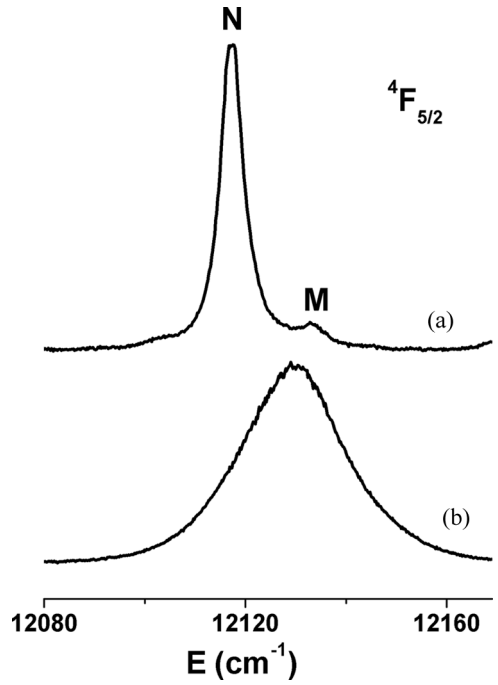

FIGURE 5 Absorption line $^4I_{9/2}(I) \rightarrow {}^4F_{5/2}(I)$ at 15 K in 0.5 at.% Nd:Sc_2O_3 ceramic (a) and (0.5 at.% Nd, 10 at.% Yb):Sc_2O_3 ceramic (b).

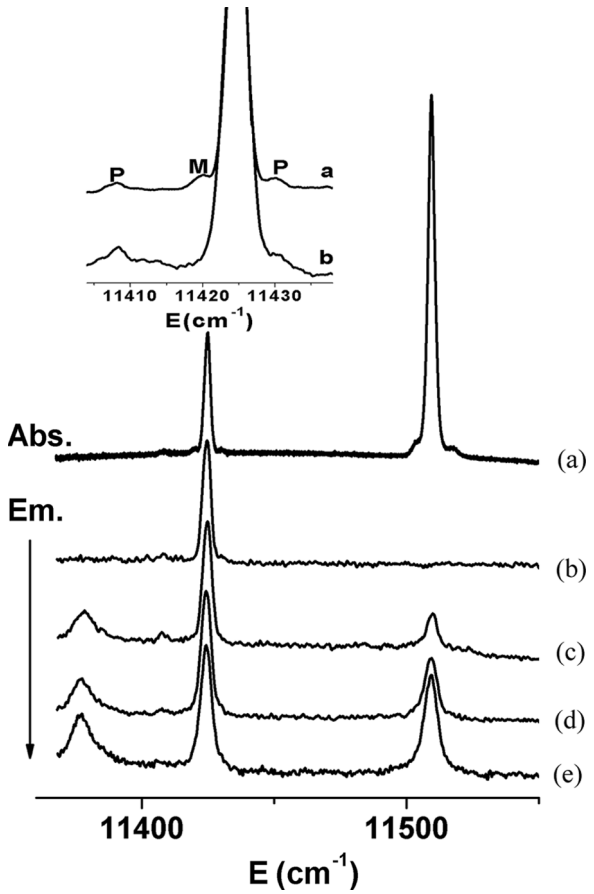

FIGURE 6 $^4I_{9/2} \leftrightarrow {}^4F_{3/2}$ absorption at 10 K (a), and l amp excited emission 10 K (b), 60 K (c), 90 K (d), 110 K (e). in l at.% Nd:YAG crystal.

give a direct picture of the relative concentrations of the various structural centers and thus provides a direct check of the distribution of perturbing centers, the luminescence spectroscopy for such transitions is a filtering experiment, the role of filter being assumed by the emission quantum efficiency. This is clearly seen by comparing the low temperature absorption $^4I_{9/2} \rightarrow {}^4F_{3/2}$ spectra of the 1 at.% Nd:YAG crystal (Fig. 6) and 2.4 at.% Nd:YAG ceramic (Fig. 7) with emission under non-selective (lamp) excitation: the satellite M_1 shows clearly in absorption but it is not seen in emission, whereas the satellites P_i, have relative emission intensity similar to absorption. This behavior is consistent with the emission quantum efficiencies for the corresponding structural centers. Similar results are obtained with short pulse selective excitation of the various centers at low temperature: with very narrow detection gate at various delays, the ratio between the emission of the M_i centers to that of the N and P_i centers diminishes in a manner consistent with the corresponding lifetimes. With very long detection gate the emission of W_1 is practically absent, whereas that of M_2 is very weak compared to the N and P_i centers whose selectively excited $^4F_{3/2} \rightarrow {}^4I_{11/2}$ emission in 1 at.% Nd:YAG crystal is shown in Fig. 8.

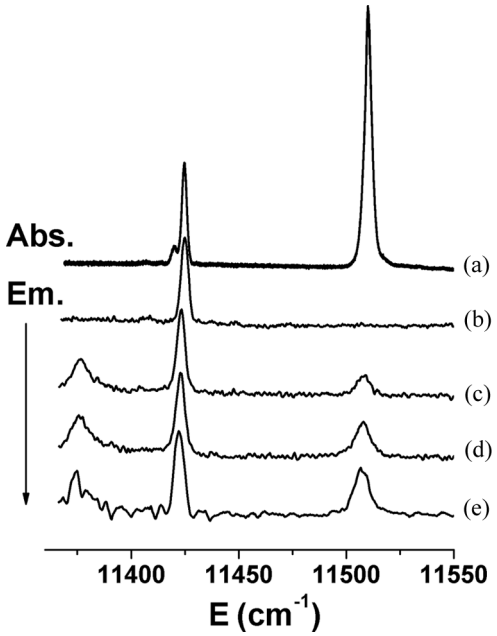

FIGURE 7 $^4I_{9/2} \leftrightarrow {}^4F_{3/2}$ absorption at 10 K (a), and lamp excited emission 10 K (b), 75 K (c), 100 K (d), 120 K (e) in 2.4 at.% Nd:YAG ceramic.

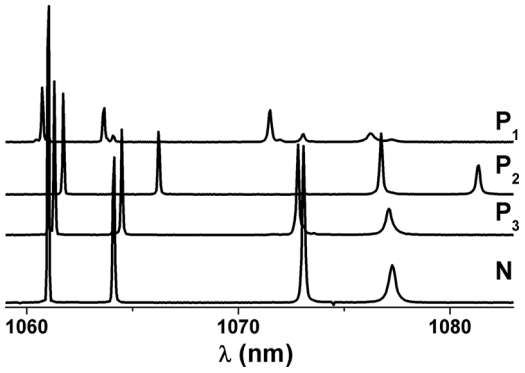

FIGURE 8 Part of selectively excited $^4F_{3/2}(I) \rightarrow {}^4I_{11/2}$ emission spectrum at 10 K for 1 at.% Nd:YAG crystal.

3.2. Systems with Charge Compensation

Several laser materials offer for substitution with RE^{3+} ions cationic sites of other valence than the doping ion. The difference of electric charge can be compensated by intrinsic defects of the host lattice (vacancies, interstitial anions) or by co-doping with foreign ions of suitable valence and this could induce structural disordering of the host lattice, the effect being influenced by the conditions of fabrication. The charge compensators can be placed far from the compensated ion and then the site occupied by the later preserves its original symmetry, or close to this ion and in this case it can perturb the crystal field leading to multicenter situation. The crystal field perturbations in this case could be much stronger than in case of the systems without charge compensation since the distortion by size effects is supplemented by the effect of difference in electric charge. Moreover, the charge compensation could induce a certain degree of correlation of placement of the compensators or of the active ions. The multicenter structure of optical spectra of the laser materials with charge compensation can give important structural information on these materials and on the charge compensation mechanism and can enable the correlation of this structure with the fabrication technology. An illustrative case is the Nd-doped $SrWO_4$ crystal, where the Nd^{3+} ions substitute Sr^{2+}. The high-resolution investigation[45] revealed major differences between the Nd:$SrWO_4$ crystals with various charge compensation mechanisms: for the crystals grown in neutral atmosphere the main charge compensation mechanism is by Sr vacancies whereas for crystals grown in air the compensation by oxygen interstitials becomes important, and in both these cases clustering of the Nd ions in n.n. or more distant Nd pairs takes place. By contrary, in case of co-doping with Na^+ the Nd ions do not cluster and two main centers, with n.n or more distant charge compensation are present.

In case of structurally disordered materials where specific crystallographic sites can be occupied by several host cations of different valence, the compensation of the difference of charge induced by doping can be accomplished by modification of the proportion of these host cations. The disorder in the cationic sites near the doping ion could induce multicenter structure and strong inhomogeneous broadening of the spectral lines, which can be used for tunable or ultrashort pulse laser emission. An interesting case is the calcium niobium gallium garnet (CNGG) where the Ca^{2+} ions occupy the large dodecahedral sites, the octahedral sites are occupied by Nb^{5+} and Ga^{3+} and the tetrahedral sites are occupied mainly by Ga^{3+}; however, this composition is non-stoichiometric and a proportion of the octahedral sites are vacant. When doping with Nd^{3+} the charge compensation can be accomplished by changing the proportion of Nb and Ga in the octahedral sites but a certain proportion of octahedral vacancies is still present, with negative effects on laser emission. This deficiency can be avoided by introducing in these octahedral sites a corresponding amount of Li^+ ions and a new compound, calcium-lithium-niobium-gallium-garnet (CLNGG) is formed, which is stoichiometric. The absorption spectra of the Nd-doped CNGG and CLNGG revealed multicenter structure of inhomogeneous broadened lines[46,47] which enabled sub-picosecond laser emission,[48] or multiple wavelength laser emission.[49] Such systems could be interesting for doping with Yb^{3+} and indeed multicenter structure of Yb:CNGG optical spectra was reported.[50] This paper reports the spectroscopic properties of Czochralski-grown Yb-doped CLNGG. The low temperature absorption spectrum of this crystal, shown in Figure 9 reveals complex multicenter structure of strongly inhomogeneous broadened bands, different from that reported for Yb:CNGG. The insert shows the decomposition of the $^2F_{7/2}(1) \rightarrow {}^2F_{5/2}(1)$ absorption line of Yb^{3+} in several components. The relative intensities of these components are analyzed in Eq. (2), assuming that

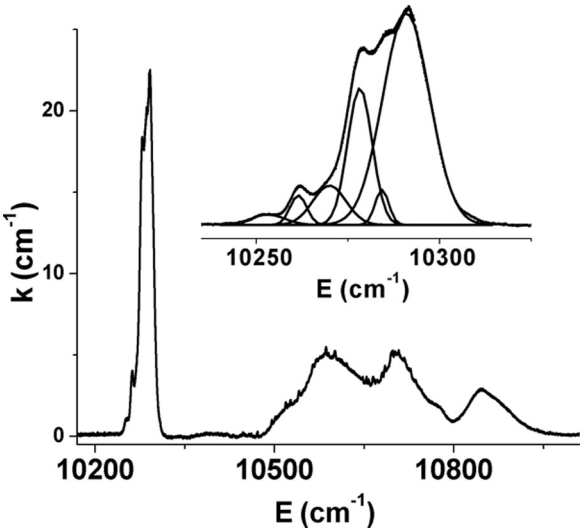

FIGURE 9 **Absorption spectrum of 4.3 at.%Yb:CLNGG crystal at 15 K. The insert shows the decomposition of the $^2F_{7/2}(1) \rightarrow {}^2F_{5/2}(1)$ absorption line in components corresponding to the various centers.**

each cationic species (Nb, Li, Ga) could occupy at random any of the octahedral sites from the n.n. coordination sphere. This analysis enables determination of the composition of this coordination sphere for each center as well as its global composition. Because the charge compensation is made by the rearrangement of the composition of Nb $^{+}$, Li^{+} and Ga^{3+}, this composition will depend on the doping concentration. In case of 4.3 at.% Yb:CLNGG crystals it was found that the majority Yb^{3+} center (62.71%) has 4 Nb^{5+} ions in the n.n. octahedral coordination sphere, followed by a center (22.61%) with vicinity $3Nb^{5+} + 1Li^{+}$, then a center (8.43%) with vicinity $3Nb^{5+} + 1Ga^{3+}$, a center (3.06%) with $2Nb^{5+} + 2Li^{+}$ and the global composition of this coordination sphere is ($Nb_{1.78}Li_{0.16}Ga_{0.06}$). Due to the multicenter structure and to the inhomogeneous broadening the absorption and emission lines remain broad at very low temperature. Luminescence with 940 nm laser diode excitation reveals broad emission lines of Yb in the temperature range from 300 K (~18 nm) to 15 K (~12 nm) that can be used for tunable or ultra-short emission at room or cryogenic temperatures.

An intermediate case is calcium gallium germanium garnet Ca3Ga2Ge3$O_1$2 (CGGG): the undoped material is ordered, i.e., the octahedral sites are occupied by Ga^{3+} ions whereas the tetrahedral sites are occupied by Ge^{4+}. However, when doped with RE^{3+} ions, which substitute Ca^{2+}, a major means of charge compensation could be the substitution of part of the tetrahedral sites by Ga^{3+}, leading to disordering. Such disorder can explain, at least in part, the complex satellite structure observed in the optical spectra of the Nd-doped CGGG[51] and the dependence of emission wavelength when pumped at various wavelengths in the absorption band.[52]

4. DISCUSSION AND CONCLUSION

The presence of multicenter structure is quite general even in laser materials that offer for doping a well defined crystallographic site and when no charge compensation is necessary. This paper infers that, despite of the fact that in most papers on laser materials the presence of the multicenter structure of the optical spectra is disregarded, such structure could provide important information on the system and could have major effects in laser emission.

In the garnet single crystals and ceramics and in cubic sequioxide ceramics doped with isovalent RE ions the multicenter structures are induced by the perturbation of the crystal field due to the association of the doping ion with specific defects of the host material (the satellites P_i in garnets) and to statistical ensembles of doping ions in near lattice sites (satellites M_i in all the considered materials). Although the crystal field perturbation reduces the crystal field symmetry at the RE^{3+} site and could modify the oscillator strength of the optical transitions, there are several transitions for which the effect can be minimized and the picture of the satellite structure reflects faithfully the relative concentrations of the corresponding centers. No additional satellites to confirm the large-scale inversion of sites between the Y^{3+} and the octahedral Al^{3+} ions[53] or presence of high concentrations of OH^{-} ions in the near vicinity of the Nd^{3+} ions to form "Nd dead sites"[54] were observed in the Nd:YAG crystals or ceramics.

The C_{RE}-independent P_i satellites are observed in the absorption and emission spectra, with lifetimes similar to the unperturbed centers N. The proportion of such defects depends on the fabrication temperature and it is quite large in the melt-grown crystals (in YAG ~1.8% of the octahedral sites are occupied by Y^{3+}) but much smaller (about one order of magnitude) in ceramics. This could induce

major differences between the melt-grown crystals and ceramics:

- The satellites P_i in the emission spectra, some with shifts as large as $16\,cm^{-1}$ from the main line could eliminate from laser emission part of the doping ions and could contribute to additional generation of heat by non-radiative de-excitation;
- A Y^{3+} ion in the octahedral Al^{3+} site introduces a relative modification of the square of local mass variation $[(M_{RE}\text{-}M)/M]^2$ that influences the heat conduction[55] by ~5.27, which is much larger than for of the substitution of Y^{3+} by Yb^{3+} (~0.9) or by Nd^{3+} (~0.39). Thus, small amounts of Y(B) centers could reduce the heat conductivity in crystals compared with the ceramics to an extent equivalent with the reduction of doping with much larger C_{RE}.
- The centers Y(B) could shift the positions of the lowest levels of the excited electronic configurations $5d4f^{n-1}$ of the rare earth ions or lower the positions of the charge transfer bands and favor the multiphoton de-excitation of the excited levels at high doping concentrations; they could also alter the emission properties of the scintillator garnet crystals.

The shift of the M satellites from the main line N depends on the mismatch between the RE^{3+} ion and the substituted host cation and on the electronic transition, the shift of the satellite M_1 being larger than for M_2. In Nd:YAG, the satellite M_1 is resolved in the low temperature absorption spectra and its maximum shift is $\sim 7\,cm^{-1}$, whereas for Nd in GSGG the shift is about half of this and the resolution is poorer. With increasing temperature the lines broaden and the shift is not able to sustain resolution. As mentioned above, earlier emission decay studies in Nd:YAG inferred that the Nd ions in the n.n. pairs that determine the M_1 satellites are coupled by mixed superexchange and dipole–dipole interactions.[12,20,40] This was subsequently challenged in the investigation of the Nd pairs in planar YAG waveguides,[56] where luminescence emission at the wavelength of satellite M_1 was reported and the energy transfer rate inside the n.n. Nd pairs inferred from the emission decay was much smaller than reported for crystals and ceramics.[12] Our new data on emission of the Nd-doped YAG and crystals and ceramics under CW non-selective excitation (tungsten-halogen lamp) or under selective pulse excitation with long detection gate show clearly the absence of emission of the M_1 satellite and confirm our earlier conclusion on the low emission quantum efficiency due to presence of superexchange coupling of the Nd ions in the n.n. pairs. The cause of the differences observed between the emission data of Nd in single crystals and ceramics and those reported for thin films is difficult to trace; a possible cause could be the presence in the thin films of non-specified amounts of other elements such as Lu or Ga, which can induce additional satellites with accidental coincidences or destroy the selectivity.

The recent 3-D investigation by confocal Raman and luminescence spectroscopy of the distribution of Nd at grain boundaries in the coarse-grained Nd:YAG ceramics evidenced sharp differences between the intensity and structure of emission of Nd near the grain boundaries and far from these.[57,58] The minimum of emission was observed at the grain boundary and from the difference between the emission line close or far from the grain boundary the presence of several spectral satellites whose relative intensities increase with the doping in the later was inferred. These satellites were assimilated to the satellites M_1 and M_2reported in the absorption spectra[12] and it was concluded that they reflect strongly increased C_{Nd} at grain boundaries, with depth of several microns; such increased C_{Nd} would induce local reduction of emission quantum efficiency and thus of the intensity of emission line N on the expense of the emission from pairs. From this it was concluded that at high C_{Nd} about 20% of the volume of the ceramic grains is affected by the Nd segregation and thus by severe emission quenching. No such effects were observed for the fine-grained ceramics.[58,59] However, there are several major points of concern in this interpretation: first, these observed satellites are much more shifted from the main line N than the satellites M_1 reported previously in the global absorption spectra of crystals and ceramics. Second, as shown by the studies on crystals and ceramics, no luminescence can be observed for the M_1 pairs, even at low temperatures or at very high Nd concentrations (9 at.%). Third, the existence of large-scale regions of enhanced Nd

concentration would modify the global emission decay of ceramics compared to the single crystals; such change was not observed either for coarse- or fine-grained ceramics.[20–23,59] Fourth, large regions of enhanced C_{Nd} would increase the global concentration of Nd pairs and modify the M satellite structure of the spectra; however, no obvious departure from the predictions of random distribution was observed in the global absorption spectra of these materials, up to high (9 at.% Nd concentrations. Fifth, no obvious lowering of performances of the lasers based on these ceramics compared with those having single crystals and which could be attributed to such large-scale Nd agglomerates was observed. Sixth, the spatial extent of the effect reported in[57,58] is much larger than the usual dept of segregation of doping ions in ceramics[60,61] which is of order of nm or even less, but it rather resembles the spatial distribution of the diffusion of impurities from the grain surfaces. It could be thus tempting to attribute the observed satellites to associations of the doping ions with local defects of the host lattice such as those induced by the use of the sintering aid based on Si, which could enter in the tetrahedral sites of garnets,[62,63] similar to the P_i satellites; the extent of the effect could be then connected with the diffusion of these defects.

The presence of the new spectral satellites in systems with several doping species (sensitized materials) enables investigation of the sensitization process and indicates that the narrow pumping properties as well as the laser emission wavelength of the activator ions in the systems with sensitization could differ from those without sensitization.

The spectral satellites in systems with charge compensation evidence the effect of compensation on the distribution of the doping ions and of compensators and the effect of technological conditions on the absorption and emission properties. In case of particular of disordered systems where specific cationic sites could be occupied by ions of different valence the multicenter structure caused by the disorder in the close vicinity of the doping ion coupled with the strong inhomogeneous broadening induced by the disorder in farther pairs leads to broad multipeaked absorption and emission bands in a large temperature range enabling efficient diode laser pumping and tunable or ultrashort laser emission.

From the cases investigated in this paper and from the data from literature it is obvious that the satellite structure in the optical spectra together with the emission dynamics is a powerful tool for investigation of the relation between the fabrication process, the structure and composition of the laser material, and the spectroscopic and laser emission properties. This relation can be then used for selection of the best conditions and parameters to optimize the laser performances (pump absorption, laser emission) and for tailoring new laser materials and laser emission schemes.

ACKNOWLEDGMENT

The research was supported by the Romanian National Agency for Scientific Research and Innovation under project IDEI-PCE 503/2009.

REFERENCES

1. Ikesue, A.; Kinoshita, T.; Kamata, K.; Yoshida, K. Fabrication and optical properties of high-performance polycrystalline Nd-YAG ceramics for solid-state lasers. *J. Amer. Ceram. Soc.* **1995**, *78*, 1033–1040.
2. Ikesue, A.; Kamata, K.; Yoshida, K. Synthesis of transparent Nd-doped HfO_2-Y_2O_3 ceramic using HIP. *J. Amer. Ceram. Soc.* **1996**, *79*, 359.
3. Lu, J.; Prabhu, M.; Song, J.; Li, C.; Xu, J.; Ueda, K.; Kaminskii, A. A. Optical properties and highly efficient laser oscillation of Nd:YAG ceramics. *Appl. Phys. B* **2000**, *71*, 469–473.
4. Ikesue, A.; Aung, Y. L.; Taira, T.; Kamimura, T.; Yoshida, K.; Messing, G. L. Progress in ceramic lasers. *Ann. Rev. Mater. Sci.* **2006**, *36*, 397–429.
5. Yagi, H.; Yanagitani, T.; Takaichi, K.; Ueda, K.; Kaminskii, A. A. Characterization and laser performances of highly transparent Nd^{3+}:$Y_3Al_5O_{12}$ laser ceramics. *Opt. Mater.* **2007**, *29*, 1251–1262.
6. Ikesue, A.; Aung, Y. L. Ceramic laser materials. *Nature Photonics* **2008**, *2*, 721–727.
7. Lupei, V. Ceramic laser materials and the prospect for high power lasers. *Opt. Mat.* **2009**, *31*, 701–706.
8. Hecht, J. New materials expand capabilities of solid-state lasers. *Laser Focus World* **2009**, *45*, 50–52.
9. Lupei, V.; Lupei, A.; Ikesue, A. Single crystal and transparent ceramic Nd-doped oxide laser materials: A comparative spectroscopic investigation. *J. Alloys. Comp.* **2004**, *380*, 61–70.
10. Lupei, V.; Lupei, A.; Ikesue, A. Transparent polycrystalline ceramic laser materials. *Opt. Mat.* **2008**, *30*, 1781–1786.
11. Lupei, V. Comparative spectroscopic investigation of rare earth doped oxide transparent ceramics and single crystals. *J. Alloys Comp.* **2008**, *451*, 52–55.
12. Lupei, V.; Lupei, A.; Tiseanu, C.; Georgescu, S.; Stoicescu, C.; Nanau, P. N. High resolution optical spectroscopy of Nd in YAG – a test for structural and distribution models. *Phys. Rev. B. Condens. Mat.* **1995**, *51*, 8–17.
13. Lupei, V. RE^{3+} emission in garnets: multisites, energy transfer and quantum efficiency. *Opt. Mat.* **2002**, *19*, 95–107.
14. Voronko, Y. K.; Sobol, A. A. Local inhomogeneity of garnet crystals doped with rare earth ions. *Phys. Stat. Sol. A* **1975**, *27*, 657–663.

15. Ashurov, M. K.; Voronko, Y. K.; Osiko, V. V.; Sobol, A. A.; Timoshechkin, M. I. Spectroscopic study of stoichiometry deviation in crystals with garnet structure. *Phys. Stat. Sol. A* **1977**, *42*, 101–110.
16. Lupei, A.; Lupei, V.; Georgescu, S.; Yen, W. M. Mechanism of energy transfer between Nd^{3+} ions in YAG. *J. Lumin.* **1987**, *39*, 35–43.
17. Lupei, A.; Lupei, V.; Osiac, E. Spectral and dynamical effects of octahedral impurities on RE^{3+} in garnets. *J. Phys. Cond. Matter* **1998**, *10*, 9701–9710.
18. Geller, S.; Fullmer, L. D.; Crandall, P. B.; Espinosa, G. P. Thermal expansion of some garnets. *Mater. Res. Bull.* **1972**, *7*, 1289–1224.
19. Brandle, C. D.; Barns, L. R. Crystal stoichiometry of Czochralski grown rare earth gallium garnets. *J. Cryst. Growth*. **1974**, *26*, 169–170.
20. Lupei, V.; Lupei, A.; Georgescu, S.; Taira, T.; Sato, Y.; Ikesue, A. The effect of Nd concentration on the spectroscopic and emission decay properties of highly-doped Nd:YAG ceramics. *Phys. Rev. B* **2001**, *64*, 092102.
21. Lupei, V.; Taira, T.; Lupei, A.; Pavel, N.; Shoji, I.; Ikesue, A. Spectroscopy and laser emission under hot band resonant pump in highly-doped Nd:YAG ceramics. *Opt. Commun.* **2001**, *195*, 225–232.
22. Lupei, V.; Lupei, A.; Pavel, N.; Taira, T.; Ikesue, A. Comparative investigation of spectroscopic and laser emission characteristics under direct 885-nm pump of concentrated Nd:YAG ceramics and crystals. *Appl. Phys. B* **2001**, *73*, 757–762.
23. Lupei, V.; Lupei, A.; Georgescu, S.; Diaconescu, B.; Taira, T.; Sato, Y.; Kurimura, S.; Ikesue, A. High-resolution spectroscopy and emission decay in concentrated Nd:YAG ceramics. *J. Opt. Soc. Amer. B* **2002**, *19*, 360–368.
24. Lupei, A.; Tiseanu, C.; Lupei, V. Correlation between spectral and structural data of YAG:Tm^{3+} and YAG:Cr^{3+}, Tm^{3+}. *Phys. Rev. B. Condens. Mat.* **1993**, *47*, 14084–14092.
25. Lupei, A.; Lupei, V.; Grecu, S.; Tiseanu, C.; Boulon, G. Crystal field levels of Tm^{3+} in GGG. *J. Appl. Phys.* **1994**, *75*, 4652–4657.
26. Tiseanu, C.; Lupei, A.; Lupei, V. Energy levels of Tm^{3+} in YAG. *J. Phys. Cond. Matter.* **1995**, *7*, 8477–8486.
27. Lupei, V.; Lupei, A.; Gheorghe, C.; Ikesue, A. Comparative high-resolution spectroscopy and emission dynamics of Nd-doped GSGG crystals and transparent ceramics. *J. Lumin.* **2008**, *128*, 885–887.
28. Chang, N. C.; Gruber, J. B.; Leavitt, R. P.; Morrison, Cl. A. Optical spectra, energy levels, and crystal fieeld analysis of tripositive rare earth ions in Y_2O_3. 1. Kramers ions in C_2 sites. *J. Chem. Phys.* **1982**, *76*, 3877–3889.
29. Leavitt, R. P.; Gruber, J. B.; Chang, J. B. Optical spectra, energy levels, and crystal fieeld analysis of tripositive rare earth ions in Y_2O_3. 2. Non-Kramers ions in C_2 sites. *J. Chem. Phys.* **1982**, *76*, 4775–4788.
30. Gruber, J. B.; Leavitt, R. P.; Morrison, C. A.; Chang, N. C. Optical spectra, energy levels, and crystal fieeld analysis of tripositive rare earth ions in Y_2O_3. 4. C_{3i} sites. *J. Chem. Phys.* **1985**, *82*, 5375–5378.
31. Petermann, K.; Huber, G.; Fornasiero, L.; Kuck, S.; Mix, E.; Peters, V.; Basun, S. A. Rare earth-doped sesquioxides. *J. Lumin.* **2000**, *87–89*, 973–975.
32. Petermann, K.; Fornasiero, L.; Mix, E.; Peters, V. High melting sesquioxides: Crystal growth, spectroscopy and laser experiments. *Opt. Mater.* **2002**, *19*, 67–71.
33. Lu, J. R.; Lu, J. H.; Murai, T.; Takaichi, K.; Uematsu, T.; Ueda, K.; Yagi, H.; Yanagitani, T.; Kaminskii, A. A. Nd:Y_2O_3 ceramic laser. *Jpn. J. Appl. Phys., Part 2,* **2001**, *40*, L1277–L1279.
34. Lupei, A.; Lupei, V.; Taira, T.; Sato, Y.; Ikesue, A.; Gheorghe, C. Energy transfer processes of Nd^{3+} in Y_2O_3 ceramics. *J. Lumin.* **2003**, *102–103*, 72–76.
35. Ushakov, S. N.; Uslamina, M. A.; Zharikov, E. V. Spectral properties of Nd^{3+} ions in samples of transparent Y_2O_3 ceramics. *Opt. Spectr.* **2009**, *106*, 549–555.
36. Lupei, V.; Lupei, A.; Ikesue, A. Transparent Nd and (Nd,Yb)-doped Sc_2O_3 ceramics as potential new laser materials. *Appl. Phys. Lett.* **2005**, *86*, 111118.
37. Judd, B. R. Optical absorption intensities of rare earth ions. *Phys. Rev.* **1962**, *127*, 750–761.
38. Ofelt, G. S. Intensities of crystal spectra of rare earth ions. *J. Chem. Phys.* **1962**, *37*, 511–520.
39. Kaminskii, A. *A. Crystalline lasers: Physical Processes and Operating Schemes*; CRC Press: Boca Raton, Fl, 1996.
40. Lupei, V.; Lupei, A.; Georgescu, S.; Ursu, I. Effects of near-neighbor pairs on energy transfer in YAG:Nd^{3+}. *Appl. Phys. Lett.* **1991**, *59*, 905–907.
41. Lupei, V.; Lupei, A. Emission dynamics of $^4F_{3/2}$ level of Nd^{3+} in YAG at low pump intensities. *Phys. Rev. B Condens. Matt.* **2000**, *61*, 8087–8098.
42. Lupei, V.; Lupei, A.; Gheorghe, C.; Ikesue, A.; Osiac, E. Energy transfer driven infrared emission processes in rare earth doped Sc_2O_3 ceramics. *J. Lumin*. **2009**, *129*, 1862.
43. Zhekov, V. I.; Murina, T. M.; Prokhorov, A. M.; Studenikin, M. I.; Georgescu, S.; Lupei, V.; Ursu, I. Cooperative processes in $Y_3Al_5O_{12}$ crystals. *Kvant. Elektron.* **1986**, *13*, 419–422.
44. Lupei, V.; Lupei, A.; Gheorghe, C.; Hau, S.; Ikesue, A. Efficient sensitization of Yb^{3+} emission by Nd^{3+} in Y_2O_3 transparent ceramics and the prospect for high-energy Yb lasers. *Opt. Lett.* **2009**, *34*, 2141–2143.
45. Lupei, A.; Lupei, V.; Gheorghe, C.; Gheorghe, L.; Achim, A. Multicenter structure of the optical spectra and the charge-compensation mechanisms in Nd: $SrWO_4$ laser crystals. *J. Appl. Phys.* **2008**, *104*, 083102.
46. Voronko, Y. K.; Sobol, A. A.; Karasik, A. Y.; Eskov, N. A.; Rabochkina, P. A.; Ushakov, S. N. Calcium niobium gallium and calcium lithium niobium gallium garnets doped with rare earth ions-effective laser materials. *Opt. Mater.* **2002**, *20*, 197–209.
47. Lupei, A.; Lupei, V.; Gheorghe, L.; Rogobete, L.; Osiac, E.; Petraru, A. The nature of nonequivalent Nd^{3+} centers in CNGG and CLNGG. *Opt. Mater.* **2001**, *16*, 403–411.
48. Xie, G. Q.; Tang, D. Y.; Luo, H.; Zhang, H. J.; Yu, H. H.; Wang, J. Y. Subpicosecond pulse generation from a Nd:CNGG laser crystal. *Opt. Lett.* **2009**, *34*, 103–105.
49. Xie, G. C.; Tang, D. Y.; Luo, H.; Zhang, H. J.; Yu, H. H.; Wang, J. Y.; Tao, X. T.; Jiang, M. H.; Qian, L. J. Dual wavelength sinchronously mode-locked Nd:CNGG laser. *Opt. Lett*. **2008**, *33*. 1872–1874.
50. Voronko, Y. K.; Popov, A. V.; Sobol, A. A.; Ushakov, S. N. Yb^{3+} ions in calcium niobium gallium garnet crystals: nearest neighbor environment and optical spectra. *Inorg. Mater.* **2006**, *42*, 1133–1137.
51. Caldino, U.; Voda, M.; Jaque, F.; Garcia Sole, J.; Kaminskii, A. A. Nd^{3+} multisites in the disordered $Ca_3Ga_2Ge_3O_{12}$ laser crystal. *Chem. Phys. Lett.* **1993**, *213*, 84–88.
52. Jaque, D.; Garcia Sole, J. Tunable Nd^{3+}:$Ca_3Ga_2Ge_3O_{12}$ site-selective laser operating around 1.33 μm. *Phys. Rev. B* **2004**, *70*, 155116 1–6.
53. Dong, J.; Lu, K. W. Noncubic symmetry in garnet structres studied using extended X-ray absorption fine structure spectra. *Phys. Rev. B* **1991**, *43*, 8808–8821.
54. Devor, D. P.; DeShazer, L. G.; Pastor, R. C. Hydroxyl impurity effects in YAG ($Y_3Al_5O_{12}$). *J. Chem. Phys.* **1984**, *81*, 4104–4117.
55. Gaume, R.; Viana, B.; Vivien, D. A simple model for the prediction of thermal conductivity in pure and doped insulating crystals. *Appl. Phys. Lett.* **2003**, *83*, 1355–1357.
56. Malinowski, M.; Nakielska, M.; Piramidowicz, R.; Sarniecki, J. Energy transfer processes in highly rare earth-doped planar YAG waveguides. *Spectrosc. Lett.* **2007**, *40*, 271–292.
57. Kochawattana, S.; Stevenson, A.; Lee, S. H.; Ramirez, M.; Gopalan, V.; Dumm, J.; Castillo, V. K.; Quarles, G. J.; Messing, G. L. Sintering and grain growth profiles in SiO_2 doped Nd:YAG. *J. Eur. Ceram. Soc.* **2008**, *28*, 1527–1534.
58. Ramirez, M. O.; Wisdom, J.; Li, H.; Aung, Y. L.; Stitt, J.; Messing, G. L.; Dierolf, V.; Liu, Z.; Ikesue, A.; Byer, R. L.; Gopalan, V. Three-dimensional grain boundary spectroscopy in transparent high power ceramic laser materials. *Opt. Express,* **2008**, *16*, 5965–5973.
59. Jacinto, C.; Benayas, A.; Catunda, T.; Garcia-Sole, J.; Kaminskii, A. A.; Jaque, D. Microstructuration induced differences in the

thermo-optical and luminescence properties of Nd:YAG fine grain ceramics and crystals. *J. Chem. Phys.* **2008**, *129*, 104705.
60. Aschauer, U.; Brown, P. Atomistic modelling study of surface segregation in Nd:YAG. *J. Am. Ceram. Soc.* **2006**, *89*, 3812–3816.
61. Aschauer, U.; Brown, P.; Parker, S. C. Surface and mirror twin grain boundary segregation in Nd:YAG: An atomistic study. *J. Am. Ceram. Soc.* **2008**, *91*, 2698–2705.
62. Boulesteix, R.; Maitre, A.; Baumard, J.-F.; Rabinovitch, Y.; Salle, C.; Weber. S.; Kilo, M. The effect of silica doping on nd diffusion in yttrium aluminum garnet ceramic: Implication for sintering mechanisms. *J. Eur. Ceram. Soc.* **2009**, *29*, 2517–2526.
63. Hollingsworth, J. P.; Kantz, J. D.; Soules, T. F. Neodymium diffusion during sintering of Nd:YAG transparent ceramics. *J. Phys. D: Appl. Phys.* **2009**, *42*, 052001.